Journal of Engineering Mathematics, Vol. 8, No. 4, October 1974
Noordhoff International Publishing – Leyden
Printed in The Netherlands

Elastodynamic analysis of crack emanating from the vertex of a wedge

V. K. VARATHARAJULU

Department of Civil Engineering, Northwestern University, Evanston, Illinois 60201, *USA*

(Received December 12, 1973)

SUMMARY

The method of homogeneous solutions is applied to the problem of elastodynamic crack propagation from the vertex of a wedge. The method is based on the observation that the particle velocity is self-similar. A closed form solution is obtained giving the shear stress and particle velocity in the vicinity of the moving crack tip. The corresponding quasi-static problem is also examined and it is found that the stress intensity factor for the quasi-static case is equal to that for the dynamic case when the velocity of crack propagation is very low compared to the shear wave velocity.

1. Introduction

When the surfaces of the wedge are subjected to spatially uniform but time-dependent shear tractions, the type of singularity generated at the vertex of the wedge is of the form $r^{1/\varkappa - 1}$, see Achenbach [1]. However, it can be shown that the singularity for the case of sudden application of anti-plane displacements is stronger and is in the form of r^{-1}. In this paper, it is assumed that this strong singularity causes the appearance of a crack at the vertex of the wedge. The crack subsequently propagates with constant velocity v into the medium in the direction symmetric to the faces of the wedge.

The shear stresses and the particle velocity in the vicinity of the moving crack tip are determined. The dynamic stress intensity factor is evaluated. Two special cases are also studied: (i) propagation of a perpendicular edge crack from a half-plane and (ii) propagation of crack in its own place. Quasi-static case is also examined and it is found that the shear stress in the vicinity of the crack tip for the quasi-static case is equal to that for the dynamic case when the velocity of crack propagation is very low compared to the shear wave velocity.

The elastodynamic problem is solved by the method of homogeneous solutions which has been extensively used in crack propagation problems (see, for example, Achenbach [2] and Achenbach and Varatharajulu [3]). The method is briefly discussed for wave propagation problems by Miles [4] and Achenbach [5]. The crucial step in the method is the application of Chaplygin's transformation which reduces the wave equation to Laplace's equation. The resulting boundary value problem is solved by the theory of complex variables.

2. Formulation of the problem

An isotropic, homogeneous, linearly elastic wedge with included angle of $2\varkappa\pi$, see Figure 1, is subjected to the following anti-plane surface disturbances:

$$\theta = 0: \qquad w = W_0 t H(t), \tag{2.1}$$

$$\theta = 2\varkappa\pi: \qquad w = -W_0 t H(t), \tag{2.2}$$

where w is the out-of-plane displacement, t is time and $H(\ )$ is the Heaviside step function. The surface disturbances generate two-dimensional horizontally polarized wave motions which are governed by

$$\partial^2 w/\partial x^2 + \partial^2 w/\partial y^2 = (1/c^2)\partial^2 w/\partial t^2, \tag{2.3}$$

where c is the velocity of transverse waves

$$c = (\mu/\rho)^{\frac{1}{2}}. \tag{2.4}$$

In (2.4) μ and ρ are the shear modulus and the mass density, respectively. The surface disturbances give rise to plane waves which propagate into the material. In addition a cylindrical wave with center at the vertex O is generated, due to the discontinuity in the boundary conditions at point O.

It can be shown by employing the method of homogeneous solutions that the discontinuity in surface displacements implied by (2.1) and (2.2) gives rise to shear stress $\tau_{\theta z}$ of the following form in the vicinity of the vertex of the wedge:

$$\tau_{\theta z} \sim \frac{2\mu W_0}{\varkappa\pi}(2ct)^{-1/(2\varkappa)} \cos\frac{\pi}{4\varkappa}\cos\frac{\theta}{2\varkappa} r^{1/(2\varkappa)-1} + \frac{\mu W_0}{\varkappa\pi r}. \tag{2.5}$$

In this paper it is assumed that the singularity given by (2.5) causes the appearance of a crack at the singular point O, at the instant that the mechanical disturbances are applied to the surfaces of the wedge. The crack subsequently propagates with a constant velocity v, where $v < c$, under an angle $\varkappa\pi$ with the surface $\theta = 0$ of the wedge. Thus at time $t > 0$ the crack tip is located at the point D, defined by $r = vt$, $\theta = \varkappa\pi$, see Figure 1. Note that P and Q denote the surface trace of the crack, but at different sides of the fracture surface. The positions of the plane wavefronts, EB and GH, and of the cylindrical wavefront, ABGF, are also indicated in Figure 1. The moving

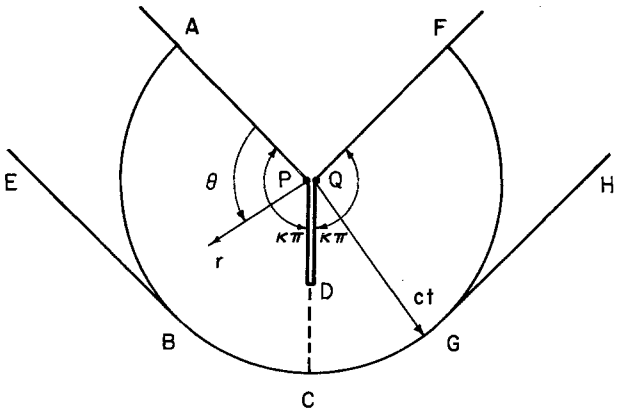

Figure 1. Pattern of wavefronts for $t > 0$.

crack tip also generates waves. However the analysis of these waves is imbedded in the wave analysis of the cylindrical wave centered at O. The problem posed, thus, requires the solution of the wave equation satisfying boundary conditions at the cylindrical wavefront centered at O and the conditions on the surfaces of the wedge and on the moving crack. The purpose of the present analysis is to compute the distributions of stresses and particle velocities inside the region of the cylindrical wave, particularly in the vicinity of the moving crack tip D.

3. Method of solution

Since the crack propagation is symmetric with respect to the surfaces of the wedge, it is enough to consider the diffracted wave pattern ABCDP, see Figure 2. The method of solutions is based on the observation that for the external disturbances that are considered here the particle velocity

$$W = \partial w/\partial t \tag{3.1}$$

is self-similar, i.e., W is a function of θ and r/t. In polar coordinates r, θ, z, the governing equation for $W(r, \theta, t)$ is

$$\frac{1}{r}\frac{\partial}{\partial r}\left(r\frac{\partial W}{\partial r}\right)+\frac{1}{r^2}\frac{\partial^2 W}{\partial\theta^2}=\frac{1}{c^2}\frac{\partial^2 W}{\partial\theta^2}. \tag{3.2}$$

Introducing a new variable

$$s=r/t, \tag{3.3}$$

the equation for $W(s,\theta)$ follows from (3.2) as

$$s^2\left(1-\frac{s^2}{c^2}\right)\frac{\partial^2 W}{\partial s^2}+s\left(1-\frac{2s^2}{c^2}\right)\frac{\partial W}{\partial s}+\frac{\partial^2 W}{\partial\theta^2}=0. \tag{3.4}$$

Within the region of the cylindrical wave ABCDP, the boundary conditions on $W(s,\theta)$ assume the following form:

$$\theta=0, \qquad s\leqq c: \qquad W=W_0, \tag{3.5}$$

$$0<\theta<\pi/2, \qquad s=c: \qquad W=W_0, \tag{3.6}$$

$$-\pi/2<\theta<\varkappa\pi, \qquad s=c: \qquad W=0, \tag{3.7}$$

$$\theta=\varkappa\pi, \qquad 0<s<v: \quad \partial W/\partial\theta=0, \tag{3.8}$$

and

$$\theta=\varkappa\pi, \qquad v<s<c: \quad W=0. \tag{3.9}$$

For $s<c$ the following transformation

$$\beta=\operatorname{arccosh}(c/s), \tag{3.10}$$

which is known as Chaplygin's transformation, reduces (3.4) to Laplace's equation

$$\partial^2 W/\partial\beta^2+\partial^2 W/\partial\theta^2=0. \tag{3.11}$$

The real transformation maps the interior of the cylindrical domain with the wedge, Figure 2, into a semi-infinite strip in the θ-β plane, see Figure 3, inside of which W satisfies Laplace's equation (3.11). The boundary conditions on $W(\beta,\theta)$ take the form as indicated in Figure 3. The harmonic function W may be written as the real part of an analytic function $F(\beta,\theta)$, i.e.,

$$W=\operatorname{Re}F(\beta,\theta). \tag{3.12}$$

The function F can, in principle, be obtained by conformal mapping techniques. Here we use the following Schwarz-Christoffel transformation which was employed by Achenbach [1]

$$\zeta=\xi+i\eta=\operatorname{sech}[(\beta-i\theta)/\varkappa] \tag{3.13}$$

to map the semi-infinite region onto the upper half of the ζ-plane, Figure 4. The boundary conditions shown in Figure 3 are converted into conditions on the real axis in the ζ-plane:

$$\xi<\xi_D=-\left[\cosh\left\{\frac{\operatorname{arccosh} c/v}{\varkappa}\right\}\right]^{-1}: \quad W=0, \tag{3.14}$$

$$\xi_D<\xi<0: \qquad \partial W/\partial\eta=0, \tag{3.15}$$

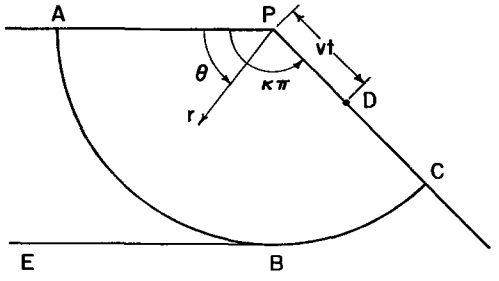

Figure 2. Pattern of wavefronts for the half wedge.

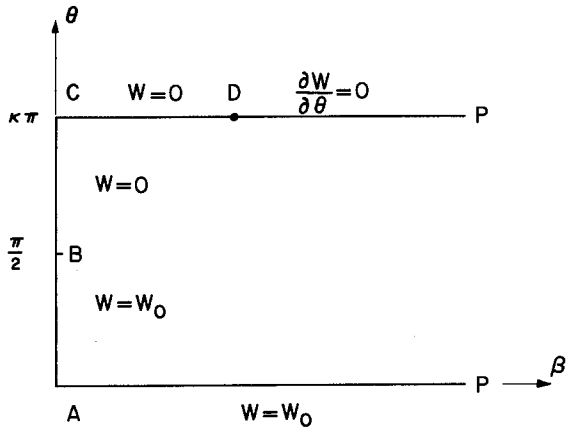

Figure 3. The θ–β plane.

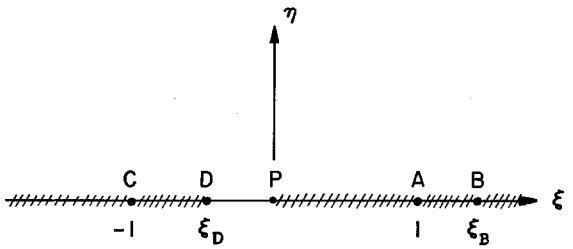

Figure 4. Mapping on the ζ-plane.

$$0<\xi<\xi_B=[\cos(\pi/2\varkappa)]^{-1}: \qquad W=W_0\,, \tag{3.16}$$

$$\xi>\xi_B: \qquad W=0\,. \tag{3.17}$$

The analytic function $F(\zeta)$ satisfying the boundary conditions (3.14)–(3.17) should now be constructed. From (3.15), we conclude that $F'(\zeta)$, where prime denotes the differentiation with respect to the argument of the function, is real in the interval $\xi_D<\xi<0$ of the real axis. Along the remaining portion of the real axis, $F'(\zeta)$ is imaginary. Also since there is a discontinuity in W at $\xi=\xi_B$, we should expect a simple pole at this point in the expression for $F'(\zeta)$. The function $F'(\zeta)$ satisfying the foregoing requirements can easily be constructed (see, for example, Muskhelishvili [6]) and is of the form

$$F'(\zeta)=iA/(\zeta-\xi_D)^{\frac{1}{2}}\zeta^{\frac{1}{2}}(\zeta-\xi_B)\,, \tag{3.18}$$

where A is a real constant. The harmonic function W may, then, be obtained as

$$W=\mathrm{Re}\left\{\int_{-\infty}^{\zeta}\frac{iA\,du}{(u-\xi_D)^{\frac{1}{2}}u^{\frac{1}{2}}(u-\xi_B)}+C\right\}. \tag{3.19}$$

The appearance of the radicals $(\zeta-\xi_D)^{\frac{1}{2}}\zeta^{\frac{1}{2}}$ in (3.18) and (3.19) requires that branch cuts must be introduced to render the expression $F'(\zeta)$ and W single valued. The condition (3.14) along the real axis in the region $-\infty<\xi<\xi_D$ shows that $C\equiv 0$. However, for $0<\xi<\xi_B$, W has a non-zero real part contributed by the integral along the semi-circular portion of the path above ξ_B. By applying the boundary condition (3.16), we find that

$$A=(W_0/\pi)(\xi_B-\xi_D)^{\frac{1}{2}}\xi_B^{\frac{1}{2}}\,. \tag{3.20}$$

The equation (3.19) with $C\equiv 0$ and A defined by (3.20) satisfies the conditions (3.14)–(3.17).

4. Stress and particle velocity fields

The relevant shear stresses in longitudinal shear motion are given by

$$\tau_{\theta z} = (\mu/r)\partial w/\partial\theta\,, \tag{4.1}$$

and

$$\tau_{rz} = \mu\partial w/\partial r\,. \tag{4.2}$$

It can be easily checked that the derivatives of these shear stresses with respect to time can be written as

$$T_{\theta z} = \frac{\mu}{r}\,\mathrm{Re}\left(\frac{dF}{d\zeta}\,\frac{\partial\zeta}{\partial\theta}\right), \tag{4.3}$$

and

$$T_{rz} = \mu\,\mathrm{Re}\left(\frac{dF}{d\zeta}\,\frac{\partial\zeta}{\partial\beta}\,\frac{\partial\beta}{\partial r}\right). \tag{4.4}$$

Employing (3.13) and (3.18) in (4.3) and (4.4), we obtain

$$T_{\theta z} = -(A\mu/\varkappa r)\cos(\pi/2\varkappa)(E_1 G_1 - E_2 G_2)\,, \tag{4.5}$$

and

$$T_{rz} = -(A\mu/\varkappa r)\cos(\pi/2\varkappa)\,ct\,(E_1 G_2 + E_2 G_1)(c^2 t^2 - r^2)^{-\frac{1}{2}}\,, \tag{4.6}$$

where

$$E(\beta, \theta, \varkappa) = E_1 + iE_2 = [1 - \xi_D \cosh\{(\beta - i\theta)/\varkappa\}]^{-\frac{1}{2}}\,, \tag{4.7}$$

and

$$G(\beta, \theta, \varkappa) = G_1 + iG_2 = \frac{\sinh[(\beta - i\theta)/\varkappa]}{\cos(\pi/2\varkappa) - \cosh[(\beta - i\theta)/\varkappa]}\,. \tag{4.8}$$

To compute the particle velocity, we observe that

$$\partial W/\partial t = (-r/t)\partial W/\partial r\,. \tag{4.9}$$

Using Eq. (3.18), we obtain

$$\frac{\partial W}{\partial t} = -\frac{r}{t}\,\mathrm{Re}\;\frac{dF}{d\zeta}\,\frac{\partial\zeta}{\partial\beta}\,\frac{\partial\beta}{\partial r}\,, \tag{4.10}$$

which can be rewritten as

$$\frac{\partial W}{\partial t} = (Ac/\varkappa)\cos(\pi/2\varkappa)(E_1 G_2 + E_2 G_1)(c^2 t^2 - r^2)^{-\frac{1}{2}}\,. \tag{4.11}$$

5. Dynamic stress intensity factor

To study the dynamic stress intensity, the shear stress near the tip of the crack must be investigated. To this end, we introduce a new set of polar coordinates (R, ϕ) as shown in Figure 5. By using trigonometric relations within the triangle, we find

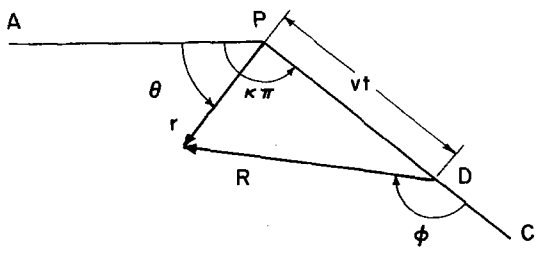

Figure 5. Polar coordinates centered at the moving crack tip.

$$\tau_{\phi z} = \tau_{\theta z} \cos\phi + \tau_{rz} \sin\phi \,. \tag{5.1}$$

From Figure 5, we get

$$\theta = \varkappa\pi - \arctan\left[R \sin\phi/(vt + R\cos\phi)\right] \tag{5.2}$$

$$r^2 = R^2 + v^2t^2 + 2Rvt\cos\phi \,. \tag{5.3}$$

In the limit of small R/vt, we can make the following simplifications:

$$\theta \sim \varkappa\pi - R\sin\phi/vt \,, \tag{5.4}$$

$$r \sim vt + R\cos\phi \,, \tag{5.5}$$

and

$$\beta \sim \beta_D + [(R/vt)\cos\phi](1 - v^2/c^2)^{-\frac{1}{2}} \,. \tag{5.6}$$

Using the expressions (5.4)–(5.6), we can write for small R/vt

$$\cos\theta/\varkappa \sim -1 + (\tfrac{1}{2})(R\sin\phi/\varkappa vt)^2 \tag{5.7}$$

$$\sin\theta/\varkappa \sim (R/vt)\sin\phi \tag{5.8}$$

$$\cosh\frac{\beta}{\varkappa} \sim -\frac{1}{\xi_D} + \frac{1}{\varkappa}\frac{R\cos\phi/vt}{(1 - v^2/c^2)^{\frac{1}{2}}}\left(\frac{1}{\xi_D^2} - 1\right), \tag{5.9}$$

and

$$\sinh\beta/\varkappa \sim (1/\xi_D^2 - 1)^{\frac{1}{2}} \,. \tag{5.10}$$

From (4.5) and (4.6), we note that the stresses depend on E and G. Hence, (4.7) and (4.8) need to be rewritten in terms of R and ϕ. Substituting the expressions (5.7)–(5.10) into (4.7) and separating the real and imaginary parts, we obtain

$$E_1 = \frac{1}{2^{\frac{1}{2}}}\left(\frac{1 - v^2/c^2}{1 - \xi_D^2}\right)^{\frac{1}{4}}\left(\frac{\varkappa vt}{R}\right)^{\frac{1}{2}}\left\{\frac{[1 - v^2/c^2\sin^2\phi]^{\frac{1}{2}} + \cos\phi}{1 - v^2/c^2\sin^2\phi}\right\}^{\frac{1}{2}}, \tag{5.11}$$

and

$$E_2 = -\frac{1}{2^{\frac{1}{2}}}\left(\frac{1 - v^2/c^2}{1 - \xi_D^2}\right)^{\frac{1}{4}}\left(\frac{\varkappa vt}{R}\right)^{\frac{1}{2}}\left\{\frac{[1 - v^2/c^2\sin^2\phi]^{\frac{1}{2}} - \cos\phi}{1 - v^2/c^2\sin^2\phi}\right\}^{\frac{1}{2}}. \tag{5.12}$$

Separating the real and imaginary parts of (4.8), we get

$$G_1 = \frac{\sinh\frac{\beta}{\varkappa}\cos\frac{\theta}{\varkappa}\left(\cos\frac{\pi}{2\varkappa} - \cosh\frac{\beta}{\varkappa}\cos\frac{\theta}{\varkappa}\right) - \cosh\frac{\beta}{\varkappa}\sinh\frac{\beta}{\varkappa}\sin^2\frac{\theta}{\varkappa}}{\left(\cos\frac{\pi}{2\varkappa} - \cosh\frac{\beta}{\varkappa}\cos\frac{\theta}{\varkappa}\right)^2 + \left(\sinh\frac{\beta}{\varkappa}\sin\frac{\theta}{\varkappa}\right)^2}, \tag{5.13}$$

and

$$G_2 = -\frac{\cosh\frac{\beta}{\varkappa}\sin\frac{\theta}{\varkappa}\left(\cos\frac{\pi}{2\varkappa} - \cosh\frac{\beta}{\varkappa}\cos\frac{\theta}{\varkappa}\right) + \sinh^2\frac{\beta}{\varkappa}\sin\frac{\theta}{\varkappa}\cos\frac{\theta}{\varkappa}}{\left(\cos\frac{\pi}{2\varkappa} - \cosh\frac{\beta}{\varkappa}\cos\frac{\theta}{\varkappa}\right)^2 + \left(\sinh\frac{\beta}{\varkappa}\sin\frac{\theta}{\varkappa}\right)^2}. \tag{5.14}$$

In the limit of small R/vt, (5.13) and (5.14) reduce to

$$G_1 = (1 - \xi_D^2)^{\frac{1}{2}}/[1 - \xi_D\cos(\pi/2\varkappa)] \,, \tag{5.15}$$

and

$$G_2 = 0 \,. \tag{5.16}$$

Substitution of the above expressions of E_1, E_2, G_1 and G_2 in (4.5) and (4.6) and subsequent

integration with respect to time t yields the shear stresses in the vicinity of the crack tip and they are

$$\tau_{\theta z} = 2^{\frac{1}{2}}\mu A\left(\frac{t}{\varkappa vR}\right)^{\frac{1}{2}} \frac{[(1-v^2/c^2)(1-\xi_D^2)]^{\frac{1}{4}}\cos(\pi/2\varkappa)}{(\xi_D\cos\pi/2\varkappa-1)} \left\{\frac{[1-v^2/c^2\sin^2\phi]^{\frac{1}{2}}+\cos\phi}{1-v^2/c^2\sin^2\phi}\right\}^{\frac{1}{2}}, \tag{5.17}$$

and

$$\tau_{rz} = -2^{\frac{1}{2}}\mu A\left(\frac{1-\xi_D^2}{1-v^2/c^2}\right)^{\frac{1}{4}}\left(\frac{t}{\varkappa vR}\right)^{\frac{1}{2}} \frac{\cos(\pi/2\varkappa)}{(\xi_D\cos\pi/2\varkappa-1)} \left\{\frac{[1-v^2/c^2\sin^2\phi]^{\frac{1}{2}}-\cos\phi}{1-v^2/c^2\sin^2\phi}\right\}^{\frac{1}{2}}. \tag{5.18}$$

Substituting (5.17) and (5.18) into (5.1), we obtain the shear stress $\tau_{\phi z}$ in the vicinity of the crack tip:

$$\tau_{\phi z} = k_\tau \Phi_\tau / R^{\frac{1}{2}}, \tag{5.19}$$

where dynamic stress intensity factor

$$k_\tau = 2^{\frac{1}{2}}\mu A \frac{[(1-v^2/c^2)(1-\xi_D^2)]^{\frac{1}{4}}\cos(\pi/2\varkappa)}{\varkappa^{\frac{1}{2}}(\xi_D\cos\pi/2\varkappa-1)}(t/v)^{\frac{1}{2}}, \tag{5.20}$$

and

$$\Phi_\tau = \left\{\frac{[1-v^2/c^2\sin^2\phi]^{\frac{1}{2}}+\cos\phi}{1-v^2/c^2\sin^2\phi}\right\}^{\frac{1}{2}}\cos\phi - \frac{1}{(1-v^2/c^2)^{\frac{1}{2}}}\left\{\frac{[1-v^2/c^2\sin^2\phi]^{\frac{1}{2}}-\cos\phi}{1-v^2/c^2\sin^2\phi}\right\}^{\frac{1}{2}}\sin\phi. \tag{5.21}$$

Employing (4.6) and (4.9), the particle velocity in the vicinity of the crack tip can easily be evaluated as

$$W \sim k_W \Phi_W / R^{\frac{1}{2}}, \tag{5.22}$$

where

$$k_W = 2^{\frac{1}{2}}\mu A\left(\frac{1-\xi_D^2}{1-v^2/c^2}\right)^{\frac{1}{4}}\left(\frac{vt}{\varkappa}\right)^{\frac{1}{2}} \frac{\cos(\pi/2\varkappa)}{(\xi_D\cos\pi/2\varkappa-1)}, \tag{5.23}$$

and

$$\Phi_W = \left\{\frac{[1-v^2/c^2\sin^2\phi]^{\frac{1}{2}}-\cos\phi}{1-v^2/c^2\sin^2\phi}\right\}^{\frac{1}{2}}. \tag{5.24}$$

For $v/c \ll 1$, i.e., when the length of the crack is very small when compared to the distance travelled by the cylindrical wavefront, we observe that

$$\xi_D \sim 0, \quad A = W_0/[\pi\cos(\pi/2\varkappa)] \quad \text{and} \quad \Phi_\tau = 2^{\frac{1}{2}}\cos(\phi/2). \tag{5.25a, b, c}$$

The shear stress $\tau_{\phi z}$ then reduces to

$$\tau_{\phi z} = \mu W_0 t\cos(\phi/2)/\pi(\varkappa lR)^{\frac{1}{2}}, \tag{5.26}$$

where $l = vt$ is the length of the crack.

Now we consider two special cases. When $\varkappa = \frac{1}{2}$, the problem reduces to the case of a perpendicular crack propagating from the surface of the half-plane. For $\varkappa = \frac{1}{2}$, we note that

$$\xi_D = -(2c^2/v^2 - 1)^{-1}, \tag{5.27}$$

and

$$\xi_B = -1. \tag{5.28}$$

Substituting (5.27) and (5.28) in (5.20), we obtain the stress intensity factor k_τ for the perpendicular edge crack:

$$k_\tau = (2\mu W_0/\pi)(t/v)^{\frac{1}{2}}. \tag{5.29}$$

When $\varkappa = 1$, the faces of the wedge coincide into a semi-infinite crack subjected to anti-plane tearing under prescribed displacements. The problem, thus, reduces to the case of a semi-infinite crack propagating in its own plane. For $\varkappa = 1$, we note from (3.14) and (3.16) that

$$\xi_D = -v/c, \quad \text{and} \quad \xi_B = \infty. \tag{5.30}$$

In view of (5.30), (5.20) gives

$$k_\tau = \frac{2^{\frac{1}{2}} W_0 \mu}{\pi c} \left(\frac{c^2 - v^2}{v}\right)^{\frac{1}{2}} t^{\frac{1}{2}}. \tag{5.31}$$

6. Solution of the quasi-static problem

In this section, let us assume that the faces of the wedge are displaced very slowly so that time enters only as a parameter. The position of the crack is shown in Figure 6, where l denotes the length of the crack. Since the crack propagates in a plane of symmetry with respect to the faces of the wedge, the displacement w vanishes in the plane of symmetry ahead of the crack tip.

The governing equation for this problem is merely Laplace's equation in W

$$\frac{1}{r}\frac{\partial}{\partial r}\left(r\frac{\partial W}{\partial r}\right) + \frac{1}{r^2}\frac{\partial^2 W}{\partial \theta^2} = 0. \tag{6.1}$$

The boundary conditions on $W(r, \theta)$ are:

$$\theta = 0, \quad 0 < r < l; \quad \partial W/\partial\theta = 0 \tag{6.2}$$

$$\theta = \varkappa\pi, \quad r > 0; \quad W = -W_0 \tag{6.3}$$

$$\theta = -\varkappa\pi, \quad r > 0; \quad W = W_0. \tag{6.4}$$

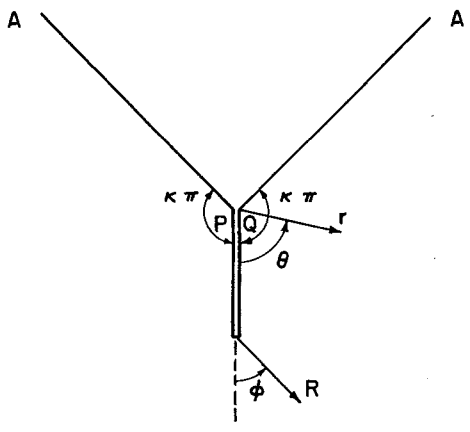

Figure 6. Cracked wedge.

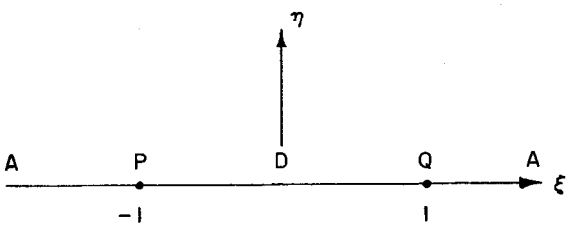

Figure 7. ζ-plane.

To solve Laplace's equation (6.1) for W, we employ an elementary conformal transformation to map the wedge with the crack onto the upper half of ζ-plane, Figure 7,

$$z = l\, e^{i\varkappa\pi}(\zeta^2-1)^{\varkappa}\,. \tag{6.5}$$

The boundary conditions on W now take the form at $\eta=0$:

$$\xi < -1\,; \qquad W = W_0 \tag{6.6}$$

$$-1 < \xi < 1\,; \quad \partial W/\partial\eta = 0 \tag{6.7}$$

$$\xi > 1\,; \qquad W = -W_0\,. \tag{6.8}$$

The analytic function satisfying (6.6)–(6.8) is clearly

$$F'(\zeta) = -i2W_0/\pi(\zeta^2-1)^{\frac{1}{2}} \tag{6.9}$$

To study the shear stress in the vicinity of the crack tip we introduce local polar coordinates R, ϕ at the crack tip D, see Figure 6. The derivative of shear stress with respect to time $T_{\phi z}$ may then be written as

$$T_{\phi z} = \frac{\mu}{R}\frac{\partial W}{\partial \phi}\,, \tag{6.10}$$

where $T_{\phi z}=\partial\tau_{\phi z}/\partial t$. It can be easily checked that (6.10) may also be expressed as

$$T_{\phi z} = \frac{\mu}{R}\mathrm{Re}\ \frac{dF}{d\zeta}\frac{\partial\zeta}{\partial z}\frac{\partial z}{\partial\phi}\,. \tag{6.11}$$

From (6.5), we compute

$$\frac{\partial\zeta}{\partial z} = -\frac{1}{2\varkappa}\left(\frac{1}{l}\right)^{1/\varkappa} z^{1/\varkappa-1}\left[1-\left(\frac{z}{l}\right)^{1/\varkappa}\right]^{\frac{1}{2}} \tag{6.12}$$

and

$$\frac{\partial z}{\partial\phi} = Ri\,e^{i\phi}\,. \tag{6.13}$$

Substituting (6.9), (6.12) and (6.13) into (6.11), employing the relation

$$z = l + R\,e^{i\phi}\,, \tag{6.14}$$

and integrating the result with respect to time t, we obtain

$$\tau_{\phi z} = \frac{\mu W_0 t}{\pi l R}\,\mathrm{Re}\left\{\frac{i\,\mathrm{Re}^{i\phi}\left[1+\dfrac{R}{l}e^{i\phi}\right]^{1/\varkappa-1}}{\left[\left(1+\dfrac{R}{l}e^{i\phi}\right)\right]^{\frac{1}{2}}\left[1-\left(1+\dfrac{R}{l}e^{i\phi}\right)^{1/\varkappa}\right]^{\frac{1}{2}}}\right\}. \tag{6.15}$$

For $R/l \ll 1$, (6.15) reduces to

$$\tau_{\phi z} = \mu W_0 t\,\cos(\phi/2)/\pi(\varkappa lR)^{\frac{1}{2}} \tag{6.16}$$

which agrees with (5.26). This means that the shear stress $\tau_{\phi z}$ for the quasi-static case is equal to that for the dynamic case when the velocity of crack propagation is very low compared to the shear wave velocity.

In conclusion, it may be remarked that the significance of the problem presented for experimental research is that it is possible to apply the loads on the surfaces of the wedge than on the surfaces of the crack. To the author's knowledge, elastodynamic experimental investigation for anti-plane case has not yet been carried out. For in-plane case, extensive experimental work has been done for the static case. The possibility of extending the static Griffith-Irwin theory of fracture mechanics in the dynamic problem of a running crack on a model of epoxy plate with central notch has been investigated by Kobayashi *et al.* [7]. Based on their study, it may

be speculated that experimental result might agree closely with the analytical work for the case when the velocity of crack propagation is substantially lower than the shear wave velocity. For higher velocities, however, good agreement may not be obtained, see [7].

Acknowledgement

This work was carried out in the course of research sponsored by the Advanced Research Project Agency of the U. S. Department of Defense and the National Science Foundation through the Northwestern University Materials Research Center. The author is indebted to Professor Jan D. Achenbach for valuable suggestions.

REFERENCES

[1] J. D. Achenbach, Shear Waves in an Elastic Wedge, *International Journal of Solids and Structures*, 6 (1970) 379–388.
[2] J. D. Achenbach, Crack Propagation Generated by a Horizontally Polarized Shear Wave, *Journal of the Mechanics and Physics of Solids*, 18 (1970) 245–259.
[3] J. D. Achenbach and V. K. Varatharajulu, Skew Crack Propagation at the Diffraction of Transient Stress Wave, *Quarterly of Applied Mathematics*, to appear.
[4] J. W. Miles, Homogeneous Solutions in Elastic Wave Propagation, *Quarterly of Applied Mathematics*, 18 (1959) 37–59.
[5] J. D. Achenbach, *Wave Propagation in Elastic Solids*, North-Holland Publishing Company, Amsterdam (1973).
[6] N. I. Muskhelishvili, *Some Basic Problems of the Mathematical Theory of Elasticity*, P. Noordhoff Ltd., Groningen, The Netherlands (1963).
[7] A. S. Kobayashi, W. B. Bradley and R. A. Selby, Transient Analysis in a Fracturing Epoxy Plate with a Central Notch, *Proceedings of the First International Conference on Fracture, Japan*, September 12–17 (1965) 1809–1831.